Title
L and M cone relative numerosity and red-green opponency from fovea to midperiphery in the human retina.

Journal
Journal of the Optical Society of America A, 17(3)

ISSN
1084-7529

Authors
Otake, S
Cicerone, CM

Publication Date
2000-03-01

DOI
10.1364/josaa.17.000615

L and M cone relative numerosity and red–green opponency from fovea to midperiphery in the human retina

Shiro Otake* and Carol M. Cicerone

Department of Cognitive Sciences, University of California, Irvine, Irvine, California 92697

Received June 23, 1999; revised manuscript received October 14, 1999; accepted October 18, 1999

The relative numerosity of the long-wavelength-sensitive (L) and middle-wavelength-sensitive (M) cones and the red–green color appearance, as assessed by means of unique yellow, are stable from fovea to midperiphery (±28 deg nasotemporal). As foveal tests decrease in size, unique yellow progressively shifts toward longer wavelengths, favoring a model of red–green opponency carried by cells whose centers receive input from either L or M cones and whose surrounds receive mixed contributions from both. Individual differences in unique yellow over a 20-nm range and the relative numerosity of L and M cones can be linked by means of this model, suggesting that the relative number of L and M cones is a factor that regulates individual variations in red–green color appearance. © 2000 Optical Society of America [S0740-3232(00)00903-0]

OCIS codes: 330.1720, 330.4060, 330.5310, 330.5510, 330.5020.

1. INTRODUCTION

There are known to be changes with retinal eccentricity in the density of the total cone population[1,2] and in the relative numerosity of the subpopulation of short-wavelength-sensitive (S) cones in the human eye.[3,4] Anatomical findings of the distribution of S cones show close correspondence to psychophysical measurements of the distribution of S cones in the human eye[5,6] and to the distribution of S cones found in nonhuman primates.[7–10] In nonhuman primates the long-wavelength-sensitive (L) and the middle-wavelength-sensitive (M) cones are estimated to be represented in nearly equal numbers,[9,10] although M cones may be more numerous than L cones in baboons.[7] A number of classical[11–13] and recent[14–20] psychophysical studies have provided estimates that favor greater numbers of L as compared with M cones in foveal and parafoveal regions in the retinas of color-normal humans, although estimates in some individuals fall below unity.[12,18] These studies provide a large range of values, including estimates in some individuals of up to nine L cones for each M cone.[18]

We address three questions in this paper. The first question is whether the relative numerosity of the L and M cones varies with retinal eccentricity in any individual retina. Hagstrom *et al.*[21] have reported that the relative amount of M-to-L cone opsin gene expression decreases with retinal eccentricity in human retina such that the value at 40 deg eccentricity is half of that measured in the central retina. In line with this report, some psychophysical studies provide indirect evidence that the relative number of L and M cones may not be stable with eccentricity. There is reported to be a marked reduction in saturation and a progressive decrease in hue discriminability (especially in midspectral regions) with increasing eccentricity.[22–25] The results of other studies[26,27] suggest that the apparent color deficiency of the extrafoveal retina may be due to changes in neural organization and not to losses in one or more of the cone types. However, recent psychophysical reports show that a full range of well-saturated hues can be observed in the extreme periphery, provided that the intensity and the size of the test stimuli are appropriately scaled with eccentricity.[28–33] In addition, the photopic luminous efficiency function does not vary with eccentricity if test fields are scaled according to the cortical magnification factor[24,34]; this suggests stability in the relative number of L and M cones, because the foveal photopic luminous efficiency function is thought to be based on a linear combination of the L and M cone spectral sensitivities weighted by their relative number.[34–36]

Estimates of the L-to-M cone ratio are stable from 28 deg nasal to 28 deg temporal eccentricity in two color-normal observers of this study. Additionally, in these same two observers, unique yellow is stable over this range of retinal eccentricities. These results are considered within the framework of a model for red–green color opponency that is dependent on two factors: the relative numerosity of the L and M cones and the relative neural weight of the center versus the surround in red–green opponent cells. The results suggest that each cone type's contribution to the red–green opponent site is the same from fovea to midperiphery.

A second question that we address concerns the center–surround neural organization for red–green opponency. We consider a model in which the surround opponency is provided purely by the class that is distinct from that which provides the center opponency and compare it with a second model in which opponency is provided by mixed L and M cone contributions to the surround. We present results showing that, as test size decreases, the choice of unique yellow progressively shifts to longer wavelengths. We argue that this result favors

a model of red–green opponent neural organization based largely on cells with mixed L and M cone inputs to surrounds.

We consider a third question, whether red–green color appearance in color normals is standardized or whether it is variable based on individual differences in features of the cone mosaic, in particular, the relative number of L and M cones. The literature survey cited above indicates that individual variability in the relative number of L and M cones may be large. There are at least two attractive proposals in the literature for ways in which color appearance among color normals might be standardized to a large degree despite individual variability in features of the retinal mosaic, such as the relative number of the different cone classes.[37–39] In this study we present an alternative model and test it against measurements of red–green color appearance. Estimates of the relative number of L and M cones and of unique yellow in a sample of 11 individuals are used to evaluate whether L and M cone relative numerosity may be linked to variability in red–green color appearance among individuals in this sample. Finally, we discuss whether this linkage may be invalidated in color-normal individuals with extreme values of the L-to-M cone ratio owing to the limited number of cones that contribute to the organization of red–green opponent neurons in foveal and near-foveal retinal regions.

2. RESULTS

A. Experiment 1: Relative Numerosity of L and M Cones from Fovea to Midperipheral Retina

There is conflicting experimental evidence of whether red–green color vision varies with retinal eccentricity, as reviewed above. Any variations in red–green color appearance with eccentricity could be due to variations in any one of at least three factors: (1) the spectral sensitivities of the L and M cone photopigments, (2) the relative number of L and M cones, and (3) neural mechanisms at the red–green opponent site. To our knowledge, there is no evidence that the relative spectral sensitivities of the cone classes vary with eccentricity in individual eyes. With regard to the second and third factors, any variations in the L-to-M cone ratio with eccentricity in an individual's retina could lead to eccentricity-dependent differences in the receptive field properties of neurons in the red–green opponent pathway unless there were compensating changes in the neural mechanisms at the opponent site. In particular, if M cone relative numerosity declines with eccentricity,[21] then without neural compensation the red–green color-opponent neurons in the periphery should reflect this decline. In turn, changes in color vision in accordance with some studies[22–25] that suggest a progression toward deuteranopia in the periphery would be expected. However, a change in the relative number of L and M cones with eccentricity need not result in changes in red–green color appearance if compensating neural factors were to act to regulate color appearance across the retina. Experiment 1 was directed at the issue of whether, in the human eye, L and M cone relative numerosity varies with eccentricity from fovea to midperiphery, a region over which recent evidence[28–33] suggests that color vision is keen. Estimates were made of the relative number of L and M cones from fovea to midperiphery (±28 deg along the nasotemporal axis) in two color-normal observers.

1. Methods

a. Observers. The observers were two color-normal males (KL, age 23 years, and SL, age 22 years), who were unaware of the purposes of the experiment. Anomaloscope matches (Neitz Anomaloscope OT) confirmed that they were color-normal trichromats. KL used contact lens corrections for myopia (−2.25 D); SL was an emmetrope.

b. Stimuli and apparatus. Measurements were made in the right eye along the horizontal meridian at the fovea centralis; at 2, 7, 17, and 28 deg temporal eccentricity; and at 2, 7, and 28 deg nasal eccentricity. (Measurements at 2 deg eccentricity were not completed for observer SL because of his time constraints.) In this range the human eye shows good off-axis optical quality, maintaining relatively constant quality with eccentricity.[40] The sizes of the stimuli were scaled to illuminate roughly the same number of cones at each eccentricity according to estimates of optical scatter[41] and anatomical estimates of cone density.[2] There is reported to be a higher density of cones in the nasal as compared with temporal hemiretina, but this difference is reported for eccentricities greater than 17 deg.[2] Because our main goal was to estimate the relative number of L and M cones at each tested location, the total density of cones should have relatively little effect. Furthermore, no measurements were made at 17 deg eccentricity in the nasal retina because of the proximity of the optic disk. The decision was made to scale the tests with eccentricity to reflect the anatomical estimates of cone density but to use the same size tests for both nasal and temporal locations at each tested eccentricity, including 28 deg, the only location likely to be affected. We expected that, if our methods were sensitive enough, a nasotemporal asymmetry in total number of cones might be detected at 28 deg eccentricity. Precision circular apertures (Newport Corporation, PH series) were used to provide test sizes corresponding to visual angles of 0.86, 1.72, 2.58, and 6.88 arc min for fovea centralis, 2, 7, 17, and 28 deg eccentricities, respectively. Test flashes were of 50-ms duration.

Stimuli were presented with a standard three-channel Maxwellian-view apparatus. One channel provided the test field, whose wavelength was controlled by a monochromator (Instruments SA Model H-20V). Interference filters (Ditric Optics) were used in the two other channels, which combined to produce the 7-deg background field. The rod-bleaching stimulus was also produced by one of these two channels. Test and background radiances were varied with neutral-density filters and wedges. A radiometer–photometer (EG&G Model 450) was used for calibrations.

As shown in Fig. 1A, for foveal tests the observer fixated the center of a (virtual) square defined by four opaque dots (diagonal separations of 2 deg) used as fixation aids. For measurements at 2 deg nasal or temporal eccentricities, the observer fixated one of three dots, with the stimulus appearing midway between the two other

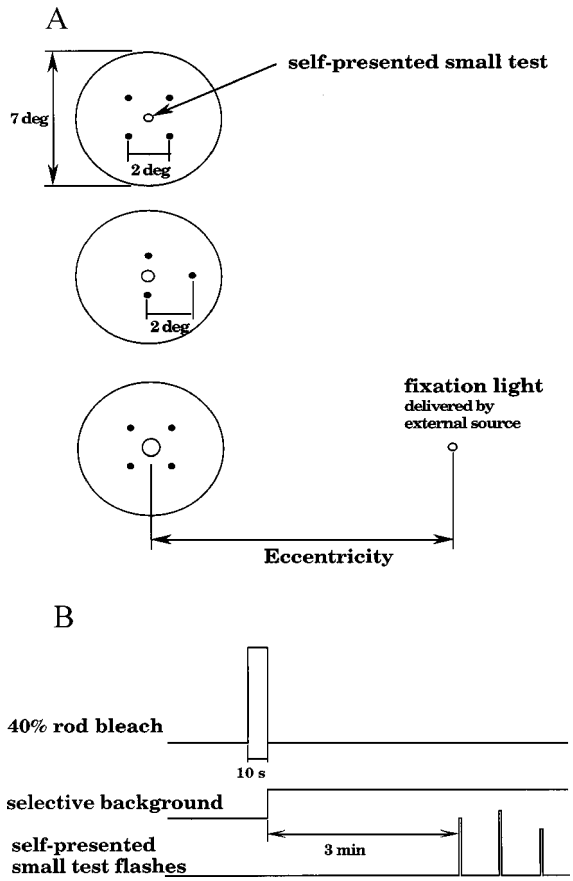

Fig. 1. A, Observer's view of foveal and eccentric presentations of the stimulus. For foveal measurements (top), the observer was asked to fixate the center of the square whose corners are marked by four dots. For measurements at 2 deg eccentricity (middle), the fixation pattern consisted of three dots in the configuration shown here or in its mirror image. The stimulus was presented midway between the two vertically placed dots. The observer was asked to fixate the third dot. For eccentricities of ⩾7 deg (bottom), the observer was asked to fixate a single fixation light delivered by a source external to the Maxwellian-view apparatus, as shown in this configuration or in its mirror image. B, Sequence of presentation of bleach, background, and test lights presented in the periphery. The bleaching light was first presented for 10 s, after which the L- or M-cone-favoring background was immediately presented. After 3 min of light adaptation, test trials were presented. Foveal measurements were identical, except that the rod bleach was not applied.

dots, located 2 deg to the right or left, respectively, of fixation and vertically separated by 2 deg. For other eccentric measurements, an external LED mounted upon a high-precision micromanipulator (Melles Griot Model 07TPD005) was used. The observer's head position was maintained with the aid of a dental impression bite bar. To further enhance fixational accuracy, observers initiated the test flash when they were sure of accurate fixation. All optical components and the bite bar were anchored to an optical table (Newport Corporation, MS series). A computer aided in the control of the experiments.

c. Procedures. The stimulus sequence is illustrated in Fig. 1B. After 10 min of dark adaptation, a 40% bleach [4.5 log scotopic trolands (td), white light presented for 10 s], producing an initial elevation in rod absolute threshold of 5 log units,[42] was applied. Immediately after application of the bleach, and before presentation of test lights, the observer light adapted to one of two background fields for 3 min until thresholds stabilized. To favor detection by M cones a 520-nm test was presented on a chromatic adapting background field composed of a mixture of 460- and 640-nm lights, chosen to reduce the sensitivity of rods, S cones, and L cones. To favor detection by L cones, measurements were made with a 640-nm test on a 500-nm background field, chosen to reduce the sensitivity of M cones as well as rods. Each background was set at a level to elevate thresholds by 0.5 log unit above the dark-adapted value, as illustrated in Fig. 2. Tests were presented for a period of 20 min after application of the bleach. If data gathering was incomplete, the sequence described above was repeated. Both M and L cone conditions were presented in each session. Four experimental sessions were conducted for each eccentricity. Each data point is based on 200 trials.

The method of constant stimuli was used. In any session, for each condition, 10 levels of test intensities in steps of 0.1 log unit were randomly presented. Ten percent of the trials were blank trials, presented randomly. The task was to place each observation in one of seven categories, corresponding to the degree of certainty that the test was seen. The observer was instructed to use the rating 0 if certain that the test was not seen, 1 if it probably was not seen, 2 if uncertain whether it was seen, 3 if it probably was seen, 4 if it was surely seen, 5 if it was surely seen and brighter, and 6 if it was surely seen and brightest. Two or three practice sessions allowed the observer to become familiar with the stimuli and the rating scale.

2. Varying Decision Criterion Does Not Bias Estimates of Cone Relative Numerosity

For estimates of the relative number of L and M cones based on yes–no detection tasks[15–17] the test is assumed to be detected if any one of the illuminated cones absorbs

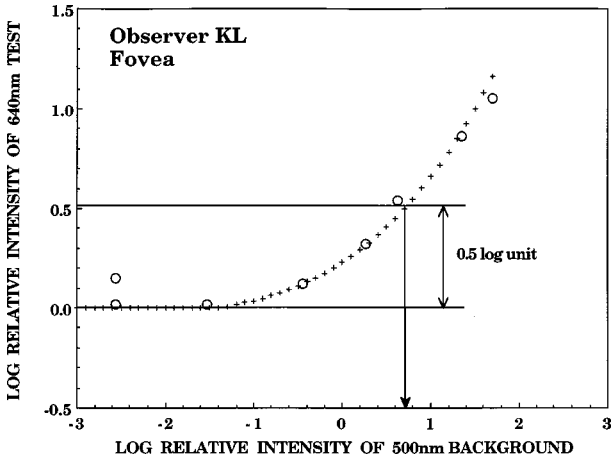

Fig. 2. Example of incremental threshold measurements used to determine the intensity of the background required for raising threshold for the test by 0.5 log unit. The data are derived from the psychometric functions defined by ratings ⩾2 (see text). Open circles, 60% seen according to this criterion. Plus signs, Stiles's theoretical threshold-versus-intensity function. The intensity of the background was chosen as that which elevated threshold 0.5 log unit above the absolute level, as indicated by the arrowhead placed on the abscissa.

the required number of quanta. To estimate the relative numerosity of different cone classes, the steepness of the psychometric function for detection based on L or M cones is related to the number of cones contributing to detection.[15] There is no clear separation of sensory from decision processes in such an analysis, and the decision criterion is thought to be rarely, if ever, exceeded by presentations of noise alone. Indeed, the observers in this study apparently adopted a high response criterion, as false alarms were virtually nonexistent (none for observer KL and one for observer SL). Nonetheless, it seemed prudent to investigate the effects of changes in the decision criterion because there is ample evidence that the observer's criterion influences the steepness of the psychometric function for test detection in rod vision[43,44] and detection of simple patterns.[45,46] The possibility that different decision criteria produce different estimates of the relative numerosity of L and M cones was discounted.

A rating procedure with seven categories representing the degrees of certainty of the presence of the signal was used to vary the decision criterion. (See details in Subsection 2.B.1.) The cumulative probability functions, defined by each of these response categories, were then evaluated after correction for guessing. The conditional probability $P(s|R_i)$, the proportion of observations placed in each rating category (R_i) on signal trials, was shown to be a monotonic function of the rating categories, indicating that the observers used the rating scale as intended.[44] Psychometric functions can be generated by use of each of the ratings as successive category boundaries (≥ 1, ≥ 2, ≥ 3, ≥ 4, ≥ 5, $=6$) and treatment of these functions as defining six different decision criteria. The psychometric functions were corrected for guessing,[46,47] and the analysis[15] used previously for yes–no data was applied to each of these functions. Briefly stated, the model specifies that a test flash that delivers an average number of quanta (x) will be detected if any one of the number (N) of illuminated cones attains a specified quantum absorption. Then the probability of detection (P) can be expressed in terms of Q, the probability that any one cone has not caught the required number of quanta, as follows:

$$P(x) = 1 - Q(x)^N.$$

What this equation expresses is that a test will be detected if any one of the N cones illuminated by the flash catches the required number of quanta. If it is assumed that the absorption of quanta in any cone follows a Poisson process, then

$$Q(x) = \sum_{k=1}^{q-1} (e^{-x}x^k/k!),$$

where q is the required number of quanta per cone to produce a particular rating. The best fit of this function to the experimental results for L cone and M cone detection determined the relative number of L and M cones.

The psychometric functions associated with the different rating categories gave values for the relative number of L and M cones that were comparable with one another, except for the categories defined by the highest ratings (≥ 5 and $=6$). For observer KL we estimated the L-to-M cone ratio as 1.99, using a criterion of ratings ≥ 2, as 2.00 using ≥ 3, and as 2.01 using ≥ 4. Hence we concluded that reasonable decision criteria produce similar estimates of the L-to-M cone ratio, and all subsequent results were based on psychometric functions generated by the cumulative responses for ratings greater than or equal to 2, a rating the observers were instructed to use if they were uncertain whether the test had been seen.

3. Estimates of the L-to-M Cone Ratio as a Function of Eccentricity

Measurements were made along the horizontal meridian at the fovea centralis, at eccentricities of 2, 7, and 28 deg in the nasal retina, and at eccentricities of 2, 7, 17, and 28 deg in the temporal retina for observer KL (Fig. 3). For observer SL, measurements were made at fovea centralis, at eccentricities of 7 and 28 deg in nasal retina, and at eccentricities of 7, 17, and 28 deg in the temporal retina (Fig. 4). The smooth curves through the data are the best-fitting functions according to the model[15] described above.

For observer KL, the relative number of L and M cones for eccentricities nasal 28, 7, and 2 deg, for fovea centra-

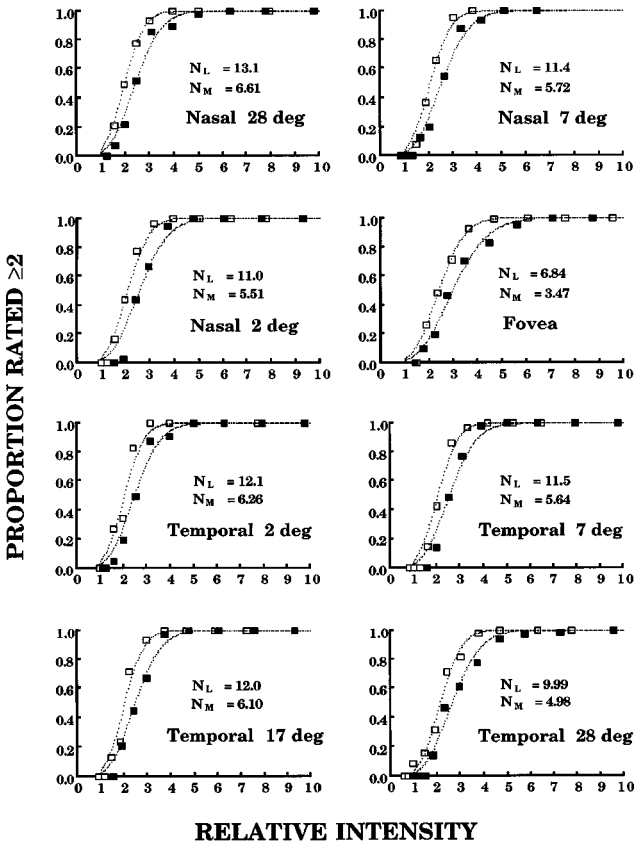

Fig. 3. Probability of detection functions for observer KL for nasal eccentricities 28, 7, and 2 deg, fovea, and temporal eccentricities 2, 7, 17, and 28 deg. Open symbols, L cone conditions; filled symbols, M cone conditions. The best-fitting theoretical functions as shown by the dotted curves (see text) were used to estimate the number of L cones (N_L) and the number of M cones (N_M) that contribute to detection at each location. The abscissa displays relative intensity in terms of a linear scale of relative numbers of quanta absorbed per cone. The nominal value of 1 displayed on the abscissa for the foveal results corresponds to an estimated value of 4.63×10^3 quanta per flash delivered at the cornea based on radiometric measurements.

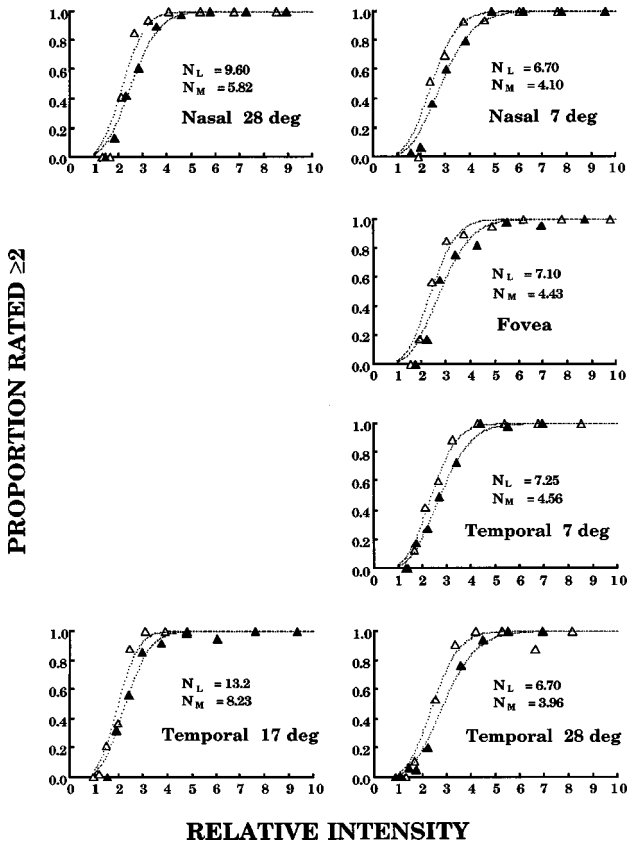

Fig. 4. Probability of detection functions for observer SL shown for nasal eccentricities 28 and 7 deg, fovea, and temporal eccentricities 7, 17, and 28 deg. Open symbols, L cone conditions; filled symbols, M cone conditions. The best-fitting theoretical functions as shown by the dotted curves (see text) were used to estimate the number of L cones (N_L) and the number of M cones (N_M) that contribute to detection at each location. The abscissa displays relative intensity in terms of a linear scale of relative numbers of quanta absorbed per cone. The nominal value of 1 displayed on the abscissa for the foveal results corresponds to an estimated value of 3.87×10^3 quanta per flash delivered at the cornea based on radiometric measurements.

lis, and for temporal 2, 7, 17, and 28 deg were 1.99, 2.00, 1.99, 1.97, 1.93, 2.05, 1.97, and 2.00, respectively, with a mean value of 1.99. For observer SL, the relative number of L and M cones at locations nasal 28 and 7 deg, fovea centralis, and temporal 7, 17, and 28 deg were 1.65, 1.63, 1.60, 1.59, 1.61, and 1.69, respectively, with a mean value of 1.63. These values are within the range of previous measurements in the fovea centralis from this laboratory.[15–17,19]

Figure 5 is a plot of the relative number of L and M cones at these various eccentricities for observers KL and SL. Standard nondirectional statistical tests for difference in slope revealed no significant difference between the best-fitting line and a line of slope zero ($p > 0.05$) for each observer.

Estimates of the cone density at the tested eccentricities can be obtained from the results of this study. We estimated the retinal areas illuminated by the test stimuli by using the optical spread function of the human eye measured at the fovea[41] and assuming an axial focal length of 16.7 mm. The estimates of the total number of cones illuminated by each test was assumed to be the sum of the estimated L cones plus the estimated M cones at each eccentricity. Figure 6 plots the estimated cone density as a function of eccentricity for observers KL and SL. The results in Fig. 6 are in reasonably good agreement with the anatomical study done by Østerberg,[1] which was based on one eye, and with that done by Curcio *et al.*,[2] which was based on four eyes.

There is reportedly a higher density of cones in the nasal than in the temporal hemiretina for eccentricities greater than 17 deg.[2] In our study no measurements were made at 17 deg eccentricity in the nasal retina because of the proximity of the optic disk. The decision was made to scale the test size with eccentricity to reflect decreasing cone density but to use the same test size for nasal and temporal presentations for a fixed eccentricity.

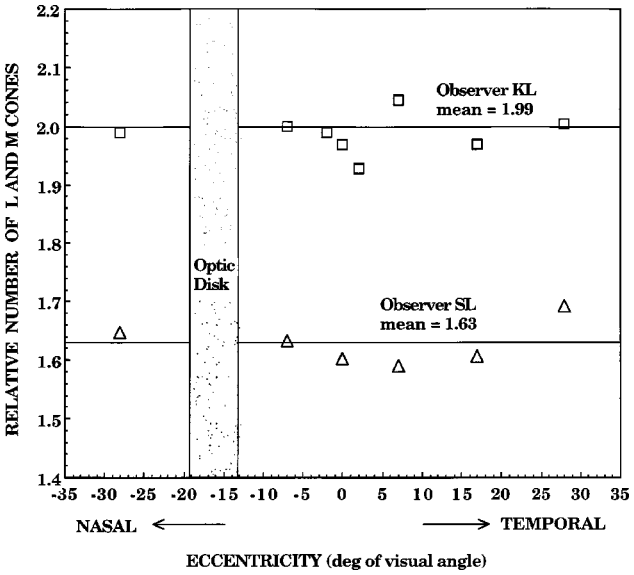

Fig. 5. Relative number of L and M cones plotted as a function of eccentricity. Squares, observer KL's results; triangles, observer SL's results. The slopes of the horizontal lines, drawn through each observer's average value, are not significantly different from zero.

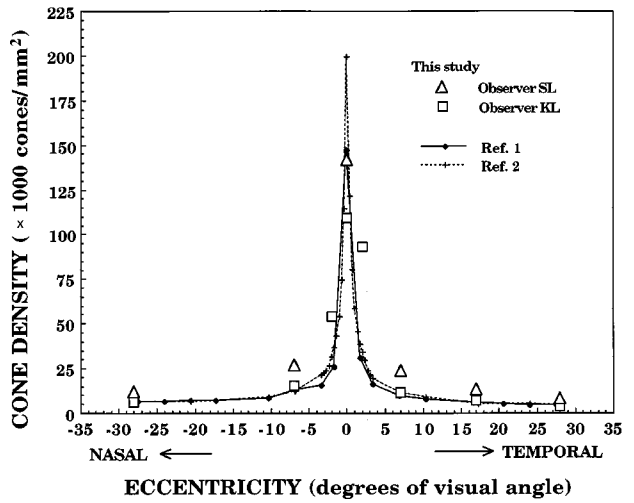

Fig. 6. Estimated density of the total number of L and M cones derived for observers KL and SL, plotted as a function of eccentricity. Also shown are the histological estimates from studies by Østerberg[1] and by Curcio *et al.*[2] for total L, M, and S cone density.

Although the estimated relative number of L-to-M cones is stable over all tested eccentricities, an indication of nasotemporal asymmetry in total numbers of cones can be seen in our results (Figs. 3 and 4 for observers KL and SL, respectively). At each location, an estimate of the total number of cones that are estimated to contribute to the detection of the test is the sum of the estimated number of L and M cones. The largest nasotemporal difference in the total number of cones is clearly that for 28 deg eccentricity. For KL the nasal value is ~20 cones, as compared with the temporal value of 15 cones; for SL the nasal value is 14–15 cones, as compared with the temporal value of 10–11 cones. This indication of a nasotemporal asymmetry in cone density in our results is compatible with that estimated by anatomical means.[2]

B. Experiment 2: Unique Yellow from Fovea to Midperipheral Retina

The results of experiment 1 indicate that the relative numerosity of L and M cones is stable from central to midperipheral retina along the nasotemporal axis at eccentricities of ±28 deg. This stability of the L and M cone relative numerosity is consistent with a stability in red–green color appearance for middle- to long-wavelength parts of the spectrum, unless there are changes as a function of eccentricity in other factors, such as the cone spectral sensitivities or the cone neural weights at the color-opponent site. To assess color appearance as a function of eccentricity, we measured unique yellow at locations corresponding to those used in experiment 1. Unique yellow is the wavelength in the red-to-green range of the spectrum for which the relative contributions made via the L and M cones to the opponent red–green color channel are thought to be balanced or in equilibrium.[48–50] Hence the measured stability in the relative number of L and M cones predicts a stability in the unique yellow wavelength with eccentricity, all else being equal. In extrafoveal locations unique yellow was measured after rod bleaches and upon the cone plateau by means of tests that were size scaled to include approximately the same number of cones at each tested eccentricity.

1. Methods

The observers and apparatus were as described for experiment 1.

Test sizes were chosen to be large enough to allow for stable judgments of color appearance (as confirmed by pilot experiments) but small enough to permit sampling from a reasonably homogeneous retinal area. Furthermore, the tests were size scaled to contain approximately the same number of cones according to anatomical estimates.[2] The sizes used were 10.3 arc min for the fovea centralis and 25.8, 43.0, 61.9, and 68.7 arc min for eccentricities, 2, 7, 17, and 28 deg, respectively. The retinal illumination of the tests was fixed at 2500 td, and the test duration was 200 ms.

After 10 min of dark adaptation a white light (4.5 log scotopic td for 10 s), estimated to bleach 40% of the rod pigment, was applied. Immediately after application of the bleach, a dim, achromatic background (173-td) field produced by a xenon-arc lamp and suitable neutral-density filters was viewed for 3 min. Three minutes after the rod bleach the cones recovered to a stable threshold, while the rod bleach in combination with the achromatic background maintained the rod threshold at a level higher than that of the cones for a period of some 20 min, during which time measurements were made. These procedures were applied at all tested eccentricities, including at the (rod-free) fovea, to provide a uniform set of testing conditions to allow for the comparison of unique yellow estimated across the retina. The observer's task was to respond either "reddish" or "greenish" to wavelengths in the yellow-appearing range presented in a staircase procedure with five randomly interleaved staircases in each session. The unique yellow wavelength was defined as that which produced 50% reddish and 50% greenish responses. The plotted values are the means of 20 different staircases over 4 sessions.

Each feature of the display—small, brief test; dim adapting background; fixation aids—was chosen for a particular purpose, as explained above. For our purposes it is not essential that unique yellow estimated by these procedures prove to be identical to that in other studies, in particular those studies that use larger test fields and no adapting background. Rather, by using tests appropriately scaled with eccentricity and the same adaptation procedures at all test locations, we sought to determine whether unique yellow varies with eccentricity. We note that foveal unique yellow estimated in this study is comparable with the values that were estimated in previous studies, one[50] conducted with a 2.6-deg, 1-s test flash on a dark background with no fixation aids and another[16] (results shown in Fig. 10 below) conducted with an 0.27-deg, 500-ms test flash on a dim background with fixation aids.

2. Estimates of Unique Yellow as a Function of Eccentricity

Figure 7 shows unique yellow measurements at locations spanning 28 deg eccentricity in nasal retina and 28 deg eccentricity in temporal retina for observers KL and SL.

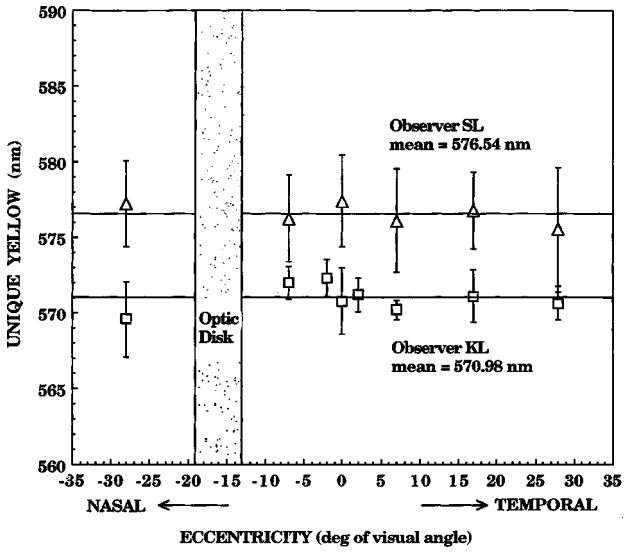

Fig. 7. Unique yellow wavelengths (±1 standard error of the mean) plotted as a function of eccentricity. Squares, observer KL's results; triangles, observer SL's results. The slopes of the horizontal lines drawn through each observer's average value are not significantly different from zero.

Consistent with the stability of the L-to-M cone ratio, the wavelength chosen as uniquely yellow is invariant as a function of eccentricity for both observers. The horizontal lines mark the average values of 571.98 nm for observer KL and 576.54 nm for observer SL. The slope of the best-fitting straight line is +0.009 for KL and −0.024 for SL. Standard nondirectional statistical tests for difference in slope revealed no significant difference between the best-fitting line and a line of slope zero ($p > 0.25$).

As noted above, the contribution of the L and M cones to the red–green opponent site depends on at least three factors: the spectral sensitivity of each cone class, the relative numerosity of each class, and the neural weighting of each class at the opponent site. *A priori*, each of these factors may vary with eccentricity and among individuals. Furthermore, significant variation in any one of these factors may be expected to produce changes in color vision unless such variation is countervailed by environmental or other factors that work to standardize color vision.[37,38] The results of experiment 1 show no significant variation in the relative numerosity of L and M cones from fovea to periphery in two color-normal observers. Experiment 2 shows, for the same two observers, that unique yellow is also unvarying over the same range of eccentricities. The results of experiment 2 support a scheme in which fovealike red–green color vision is maintained into the midperiphery and suggest that this stability may be based on the maintenance of the relative numerosity of L and M cones over the same retinal extent. These results are consistent with recent findings that suggest that a full range of well-saturated hues can be observed even in the extreme periphery, provided that the intensity and the size of the test stimuli are appropriately scaled.[27–32]

C. Experiment 3: Red–Green Opponency and the Organization of Foveal Receptive Fields

Many models of red–green color appearance are based implicitly on receptive fields organized with a strict segregation of inputs from either L or M cones to the center and from the other class to the surround. In this section we present experimental results that suggest instead that red–green opponency is based on cells with mixed contributions from L and M cones to surrounds.

In the primate retina, red–green opponency is thought to be carried by the midget ganglion cell of type 1 and the parvocellular laminae of the lateral geniculate body.[51] There are a number of unresolved details of the retinal connectivity on which the midget ganglion cell receptive field is based, and, indeed, it is an open question whether a ganglion cell type other than this one might be the primary carrier of red–green opponency.[52,53] Nonetheless, the midget ganglion cell of type 1 remains a prime candidate for conveyance of red–green signals. Two models of the type 1 red–green receptive field are currently considered feasible. In one, the selective surround model, the surround is fed exclusively by the cone class different from that which provides the center[54,55]; in the second, the mixed surround model, the surround is provided by a mixed input of L and M cones.[56–58] Regardless of which model is considered, it is reasonable to assume that the responses of all illuminated midget ganglion cells, pooled at higher sites in the color pathway, form the basis for red–green color appearance and, in particular, the determination of unique yellow. Red–green color appearance for large test fields should reflect the integration of all illuminated red–green opponent ganglion cells. As test fields are reduced in size, they may incompletely illuminate groups of cones that normally provide inputs to particular ganglion cells. Distinct predictions of changes in color appearance with reductions in test size can be made, depending on which of these two models of midget ganglion cell receptive field organization is considered.

If surrounds are selective and are fed by the cone class that is different from the one that feeds the center, L-center as well as M-center cells are equally efficient in coding red–green color information. In accordance with the results in the literature, let us assume that the L cones are more numerous than the M cones in the fovea and, therefore, that L-center cells are more numerous than M-center cells. An L-center cell is more likely to draw from distant M cones for its surround, whereas an M-center cell should be able to draw from nearby L cones for its surround. For large test fields, large numbers of L-center and M-center cells are illuminated, and the relative number of these cells should reflect the relative population of L and M cones. It is reasonable to expect that, as test size is reduced, the L-center cells are more likely to be compromised: Illumination may fall upon an L cone feeding an L-center cell, but the more distant M cone supplying the receptive field surround may not be illuminated. In this case the L-center signal is effectively enhanced because of the lack of M cone opponency. On the other hand, illuminated M-center cells should tend to respond as usual because, as noted above, nearby L cones are likely to provide the cell's surround. If so, then the red–green signal to central color sites may be overweighted toward the red for smaller than for larger fields. Thus the wavelength selected as unique yellow for a large field is predicted to tend to look too red if it is seen as a small field, and unique yellow is predicted to shift toward shorter wavelengths when it is estimated with small fields.

A different prediction is made if surrounds are mixed instead of selective. It is reasonable to expect that the larger the L-to-M cone ratio, the more likely that—for both M-center and L-center midget ganglion cells—surrounds are dominated by L cones. Thus L-center cells in an L cone rich retina would not code red–green color signals as efficiently as the M-center cells whose surrounds are provided predominantly by L cone contributions. As test size decreases, it might be expected that, for M-center cells near the margins of illumination, contributions to the surround from other, distant M cones should be reduced, thereby enhancing the central M cone response. Hence the mixed surround model leads to the predictions that the unique yellow wavelength selected for a large field should look too green when it is viewed as a small field and that the small field unique yellow should show a shift toward longer wavelengths.

1. *Methods*

The methods were as described in experiment 2 for the fovea, with the following exceptions: The observers were

two color-normal males (VC and MS), who were unaware of the purposes of the experiment. Anomaloscope matches (Neitz Anomaloscope OT) confirmed that they were color-normal trichromats. Test sizes were 3, 6, 10, 30, and 60 arc min. All tests were centered at the fovea with the fixation aid illustrated at the top of Fig. 1A.

2. Estimates of Foveal Unique Yellow as a Function of Test Size

Red–green color judgments as a function of wavelength for tests of diameters 3, 10, 30 arc min are shown in Fig. 8 for observers VC and MS. As test size decreases, fixed wavelengths are judged to be progressively greener. For example, observer MS judges 590 nm to be red on all trials when they are seen as a test of 30 arc min, but this same wavelength is judged to be green on roughly 35% of trials if they are seen as a test of 10 arc min and green on 100% of the trials if they are seen as a test of 3 arc min. Figure 9 plots the unique yellow wavelengths—those wavelengths judged red (green) on 50% of trials—as a function of test size. For observer VC, unique yellow for larger fields (30 and 60 arc min) is roughly 575 nm and shifts to longer wavelengths by as much as 10 nm for smaller test sizes. Observer MS chooses 583 as unique yellow for test sizes from 10 to 60 arc min and progressively longer wavelengths for test sizes less than 10 arc min.

These results tend to favor the mixed surround model of red–green opponency. Although the retinal circuitry that is responsible for the receptive fields of midget ganglion cells is not fully understood, other evidence supports

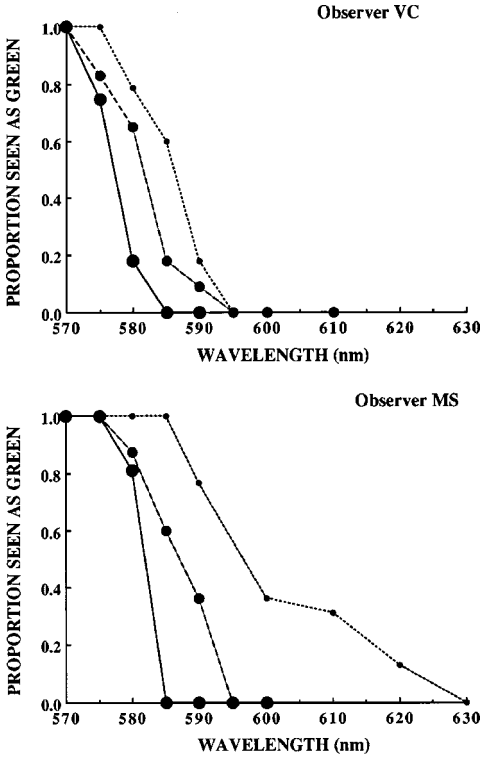

Fig. 8. Proportion of test lights of a given wavelength judged to appear green as a function of wavelength plotted for observers VC and MS. The smallest circles represent the results for a 3-arc-min test; the medium-sized circles, for a 10-arc-min test; and the largest circles, for a 30-arc-min test.

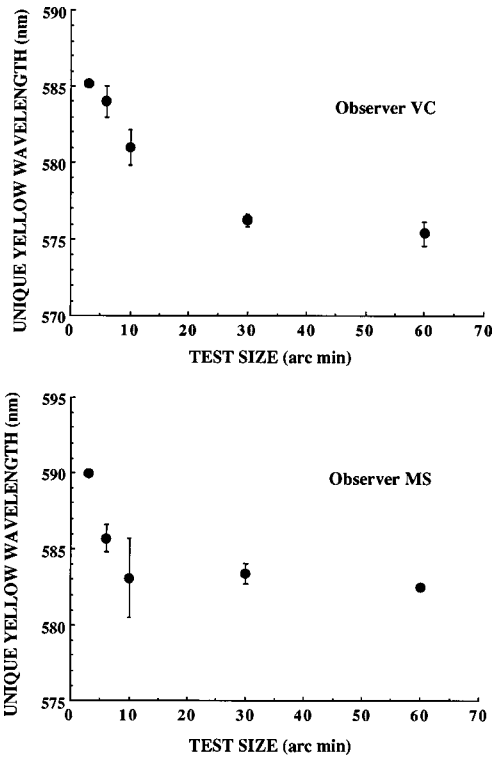

Fig. 9. Unique yellow (the wavelength judged green 50% of the time and red 50% of the time) plotted as a function of test size ranging from 3 to 60 arc min for observers VC and MS.

this model. In foveal and near-foveal regions of the retina, each midget bipolar cell is fed by a single cone,[59] and, in turn, each midget ganglion cell is fed by a single midget bipolar cell.[60] Furthermore, each cone receives processes from three to four H1 horizontal cells, each of which receives nonselective inputs from two M or L cones.[61] As one possibility, if H1 cells act to reduce the transmembrane potential of the cones that they contact, then each midget ganglion cell receives input from a single cone for its center response and nonselectively from as many as six to eight other L and M cones for its surround response.

Clearly, all of color appearance cannot be explained by this or any other model set at the level of the ganglion cells. Rather, we propose that ganglion cells, as we describe here, convey red–green signals to higher sites in the color pathway and that, regardless of the nature of further neural processing at higher sites, these ganglion cells help form the basis for red–green color appearance.

D. Model of Red–Green Opponency and Color Appearance

It is an open question whether red–green color appearance is standardized in color normals or whether it shows individual variability based on features of the cone mosaic, in particular, the relative numerosity of L and M cones. There is now a preponderance of evidence that in the human retina the L cones are more numerous than the M cones.[15–20] Moreover, individual variability in the relative number of L and M cones appears to be large, with values as high as nine L cones for each M cone.[18] Furthermore, the L and M cones appear to be randomly

arrayed[19,20] within the photoreceptor mosaic. In this subsection we consider whether this large range in the relative number of L and M cones and their random placement within the photoreceptor array might have an effect on individual variability in color appearance.

There are a number of attractive proposals in the literature for ways in which color appearance among color normals might be standardized to a large degree, despite individual variability in features of the retinal mosaic, such as the relative numbers of the different cone classes. One idea, proposed by Pokorny and Smith[37] and by Mollon,[38] specifies that the spectral position of unique yellow is the wavelength that produces the same relative quantum catch in the L and M cones as does the average environmental illuminant. According to this idea, individual variability in the relative numerosity of the cone classes and individual variability in the L and M cone photopigments are not related to color appearance. Thus, under this hypothesis, individual variability in color appearance, for example as gauged by estimates of unique yellow, should be minimal. An alternative proposal by MacLeod[39] is that compensating neural connections render color appearance nearly identical for all observers regardless of any variability in the cone spectral sensitivities or the cone relative number. The appeal of these proposals is that color appearance is standardized for color-normal observers.

According to an alternative hypothesis,[16] color appearance is not identical for all observers and, in particular, unique yellow, the equilibrium hue for red–green opponency, varies among individuals in a way linked to the relative number of L and M cones. This hypothesis is consistent with the well-documented 20-nm range[48,50,62–66] in the choice of unique yellow among color normals. In this section we report the results of testing the predictions of a mixed surround model for red–green opponent receptive fields, the model favored by the results of experiment 3, against measurements of unique yellow and the L-to-M cone relative numerosity for eleven observers (the four observers of this study and seven others[16] investigated in our laboratory).

It is important to note that these ideas need not be mutually exclusive. Clearly, individual differences exist, but standardization toward a norm may also play a role in color appearance. Indeed, nothing in this study can exclude the possibility that mechanisms[37–39] for standardization of color appearance, as noted above, are also at work in the color pathway. Rather, the development in this section is designed to establish that a reasonable model of color appearance can be based on individual differences in the relative number of the cone classes in the human retina. Such a model, we show, can explain much, but not all, of the range in unique yellow among color normals. Other factors than these two that may play a role in determining color appearance are discussed below (Subsections 3.B and 3.C).

Experiments 1 and 2 indicate that the relative numerosity of L and M cones can be directly linked to red–green color appearance from fovea to midperiphery in an individual's retina. Experiment 3 suggests that the foveal receptive fields that carry red–green opponency do so via a neural organization with mixed L and M cone inputs to surrounds. For a typical ON-center cell this can be expressed as

$$c\mathbf{M}(\lambda) - [\, j\mathbf{L}(\lambda) + k\mathbf{M}(\lambda)], \tag{1}$$

where $\mathbf{L}(\lambda)$ and $\mathbf{M}(\lambda)$ represent the cone spectral sensitivities and c represents the relative neural weight for the center as compared with the surround. The center is provided by a single M cone,[59,60] and j and k represent the number of L and M cones, respectively, that contribute to the surround. In this formulation, on average over all such cells, j/k represents the relative numerosity of the L cones as compared with the M cones, assuming that the total number of cones that contribute to the receptive field surround, $j + k$, is large enough. (In the discussion below we discuss the effect of large values of the L-to-M cone ratio on the relative contributions of L and M cones to surrounds.) Without loss of generality, we can set $k = 1$. Then, for λ_Y, the unique yellow wavelength,

$$(c - 1)\mathbf{M}(\lambda_Y) - j\mathbf{L}(\lambda_Y) = 0. \tag{2}$$

This expression describes the relationship among unique yellow (λ_Y), the relative numerosity of L and M cones (j/k), and the relative neural weight (c) for contributions to the center versus the surround in red–green opponent cells. Assuming that neural weight c is unvarying among individuals, Eq. (2) states that unique yellow, and by implication red–green color vision, varies among color normals directly according to the relative numerosity of L and M cones.

It is immediately apparent that this model predicts that individuals with higher L-to-M cone ratios should tend to choose shorter unique yellow wavelengths, given that the λ_{max} of the M cone pigment lies well short of unique yellow. Figure 10 plots unique yellow as a function of the relative number of L and M cones for 11 individuals studied in this laboratory, including the 4 individuals who participated in this study. In this sample of color-normal observers the range of L-to-M cone ratios was approximately 1.6–2.5, with a corresponding range for unique yellow of roughly 568–583 nm. As expected,

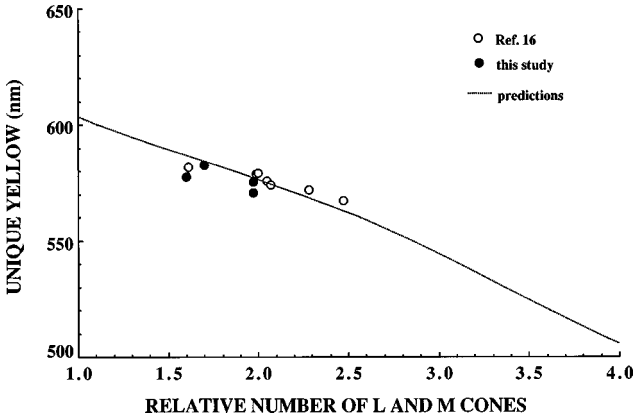

Fig. 10. Unique yellow plotted as a function of the relative number of L and M cones for foveal measurements in 11 observers [4 observers from this study (filled circles), and 7 from a previous study[16]]. The predictions are from the model described in the text [Eq. (2)]. A relative weight of center versus surround of 3.8 for the red–green opponent receptive fields best describes these results.

individuals with higher L-to-M cone ratios tend to choose shorter unique yellow wavelengths.

The best fit to the results plotted in Fig. 10 is obtained with $c = 3.8$ as the relative weighting of center to surround. According to the proposed model, the range of 568–583 nm in unique yellow is consistent with a range of L-to-M cone ratios among color normals spanning roughly 1.7–2.7, assuming that this is the only source of individual variability in red–green color opponency. It can be seen that the relationship between unique yellow and the relative numerosity of L and M cones for the individuals in this study conforms reasonably well to the proposed model. The proposed model differs from an earlier version[16] in that there is an explicit link to the higher weight accorded to center than to surround of red–green opponent cells. The relative contribution of the L cones as compared with the M cones can be expressed as $j/(c - 1)$ for $k = 1$. This value ranges from 0.61 to 0.96 for the 11 observers whose results are shown in Fig. 10.

The development thus far specifies how two factors, the relative numerosity of L and M cones and the cone neural weights at the opponent site, help to regulate red–green color vision. Furthermore, the proposed model directly links the relative cone neural weights to the preferential weighting of center as compared with surround of midget ganglion cells. The remaining factor in this model is the variability in cone pigment, λ_{max}. Current estimates of the individual differences in L and M cone pigment λ_{max} (Refs. 67–69) indicate a range of no more than 6 nm, not sufficiently large to account for the 20-nm range in unique yellow among individuals. We do not have estimates of the cone pigment spectral sensitivities in any of the individuals of our study. Thus we can only point to this factor and the possibility that it may explain the remaining variability that is unaccounted for by the model represented by Eq. (2) and displayed in Fig. 10. A more-detailed evaluation of variability in λ_{max} among individuals is deferred to Section 3.

We note that, based on Eq. (2) alone, individuals with extreme values of L and M cone relative numerosity might be expected to choose unique yellow outside the range in the literature. In Section 3 below we consider such individuals and suggest a way in which the limited extent of foveal receptive fields can provide an automatic normalization of red–green color appearance by imposing a limit on the number of cones that contribute to the receptive field surround, even for extreme values of L and M cone relative numerosity.

3. DISCUSSION

A. Color Perception in the Periphery

Unlike the results of earlier experiments for which changes in color vision with eccentricity among color-normal trichromats were reported,[22–25] recent reports show that one can achieve fovealike color vision in the periphery at eccentricities up to 40 deg by increasing stimulus size for peripheral measurements.[30] Some studies, based on hue cancellation with humans[31] and the activity of color-opponent ganglion cells in primates,[70] describe a complex pattern with stable color vision up to approximately 20 deg eccentricity but increasing L cone contribution beginning at approximately 30 deg eccentricity. In good agreement with recent psychophysical assessments of red–green color vision, the results of the present study show a stability in the relative numerosity of L and M cones as well as of the unique yellow wavelength from fovea to nasal and temporal midperiphery (28 deg eccentricity) when measurements are made with test stimuli scaled according to cone density at each eccentricity. The results of the present study show no changes in unique yellow or in the relative numerosity of L and M cones at 28 deg eccentricity in nasal and temporal retina as compared with the fovea, contrary to the expectations based on reports of a relative decrease in M cone opsin expression[21] and a relative increase in the contribution of L cones[31,70] for similar midperipheral locations.

B. Individual Variability in Cone Spectral Sensitivities and Unique Yellow

The derivations of the cone neural weights and coefficients were based on the assumption that the L and M cone spectral sensitivities are the same for the observers used in this study. This assumption is tenable in view of recent results in the literature that support only modest variation in the photopigment spectral sensitivities among individuals. Measurements of photocurrents from the isolated outer segments of individual cones show that there is little within- or between-individual variability (standard deviation of 1.5 nm) in the absorption characteristics of human cones of a given class.[68] In accordance with this finding, there is reported to be a modest difference of 4.3 nm in λ_{max} of two L cone pigment absorption spectra derived with photobleaching in tissue culture cells transfected with DNA clones of human genetic material.[69] These measurements, indicating a modest range of differences in the cone pigments among individuals, are generally consistent with conclusions from psychophysical studies, yielding estimates of little[67] or modest[71–74] variability for the range of λ_{max} differences in any cone class among color-normal individuals. However, results from microspectrophotometry[75,76] are consistent with a larger variability of 10–12 nm in the peak absorption of L as well as M cone photopigments.

Can the 20-nm range in unique yellow recorded in the literature[48,50,62–66] be explained on the basis of variations among individuals in the L or M cone pigments? Even sizable shifts in the L cone pigment λ_{max} produce little change in the predicted value of unique yellow because over this range of wavelengths the L pigment spectral sensitivity is relatively flat. For example, a shift of +9 nm in λ_{max} of the L cone pigment is calculated to produce a change toward shorter wavelengths of 1 nm in unique yellow, and a shift of −9 nm is calculated to produce a change toward longer wavelengths of 5 nm. Thus variability in the L cone pigment alone cannot account for the full range of variability among color-normal observers in the locus of unique yellow. If one considers the variability in the spectral sensitivity of the M cone pigment alone, accounting for the entire range (568–588 nm) of variability in unique yellow among color-normal observers requires a range of −7 to +9 nm in λ_{max}. Such a 16-nm range is larger than the largest reported in the literature as reviewed above. Hence individual variability in cone

photopigment spectral sensitivities—even when one considers the combined effect of variations in both L and M cone pigment λ_{max}—is not likely to be the sole determinant of individual variability in red–green color appearance as measured by unique yellow. On the other hand, it is large enough to account for the departures from the predictions of the model proposed in this study (Fig. 10).

C. Extreme L and M Cone Relative Numerosity and Red–Green Color Appearance

The model proposed above links L and M cone relative numerosity and red–green opponency in the fovea. The model predicts a range for unique yellow that approximately matches the range recorded in the literature for color-normal observers and that also matches the results from 11 color normals tested in this laboratory (Fig. 10). The development in this study establishes that a reasonable model of color appearance can be based on individual differences in the relative number of the cone classes in the human retina. Note that nothing in this study can exclude the possibility that mechanisms[37–39] for standardization of color appearance as noted above are also at work in the color pathway. Indeed, there are reports of observers with extreme L-to-M cone ratios who nonetheless select unique yellow within this normal range. For example, heterozygous carriers for X-linked color-vision deficiencies with extreme L-to-M cone ratios are reported to show no differences in judged red–green color appearance as compared with color-normal individuals.[77,78] These findings of a dissociation between unique yellow and the L-to-M cone ratio support the possibility that the spectral position of unique yellow may depend on factors other than the relative number of L and M cones.[37–39]

Can the model proposed in this paper (Subsection 2.D) provide an alternative account for such observers? If the green–red signal is carried by means of opponency between receptive field center and surround, a kind of normalization of this signal is automatically imposed by the limitations of the inputs to the midget ganglion cell. There are two ways in which this point can be argued. First, it is estimated that in foveal and near-foveal regions the dendritic spread of midget ganglion cells is of the order of 4–5 μm,[60] extending over roughly 1 arc min, a range estimated to include some seven cones. Second, each midget ganglion cell in foveal and near-foveal regions receives input from a single midget bipolar cell,[60] which is fed by a single cone.[59] Each cone receives processes from 3–4 H1 horizontal cells, each of which receive inputs from two M or L cones in this region of the retina.[61] In this case, if H1 cells act to reduce the transmembrane potential of the cones that they contact, then each midget ganglion cell receives input from a single cone for its center response and potentially six to eight other cones for its surround. Thus, in either case, a single L or M cone provides the center of a midget ganglion cell, and at most six to eight L and M cones contribute to its surround. This would be the case regardless of how high the L-to-M cone relative numerosity might be. We suggest that this is a mechanism that ensures that red–green color appearance is somewhat standardized in trichromats, consistent with the 20-nm range of unique yellow found in the literature.

It should be noted that, for extreme L-to-M cone ratios that are less than unity, the same arguments hold. In this case M-center cells are not capable of effectively carrying a red–green opponent signal, because their surrounds are likely to be composed largely of M cone inputs. L-center cells, on the other hand, could effectively convey red–green opponency by virtue of the relatively larger number of M cones as compared with the number of L cones that compose their surrounds. Additionally, the total number of L and M cones that contribute to the surround would again be at most eight by the argument made above.

D. Cone Contributions at the Red–Green Opponent Site

Estimates based on contrast detection tasks[79] and grating detection tasks[80] are in agreement that detection by means of the red–green mechanism depends on equally weighted differences of the L and M cones. If, as has been argued,[81] the red–green detection mechanism is identical to the red–green color-opponent mechanism, our estimates of the cone contributions at the color-opponent site should match the estimates based on detection. The results of this study yield a value of the ratio of L cone contribution to M cone contribution at the red–green opponent site [see Eq. (2)] as ranging from 0.61 to 0.96 for the 11 observers described in Fig. 10. Hence, in our results, although some observers provide estimates of equal weighting of the L and M cone contributions to red–green color appearance, most observers yield a value below unity. The color appearance task of the present study and a detection task may not be processed in the same way by the color-opponent pathway, raising the possibility that, as compared with contrast or grating detection, color appearance for suprathreshold lights is regulated at a different point in the color–opponent pathway.

ACKNOWLEDGMENTS

S. Otake's visit to this laboratory was supported by Matsushita Electric Industrial Company, Ltd. This study was supported by National Institutes of Health grant EY-11132 to C. M. Cicerone.

C. M. Cicerone's e-mail address is cciceron@uci.edu.

*Present address, Corporate Research Division, Matsushita Electric Industrial Company, Ltd., 3-4 Hikari-dai, Seika, Soraku, Kyoto 619-02, Japan.

REFERENCES

1. G. Østerberg, "Topography of the layer of rods and cones in the human retina," Acta Ophthalmol. Suppl. **6**, 1–102 (1935).
2. C. A. Curcio, K. R. Sloan, Jr., O. Packer, R. E. Kalina, and A. E. Hendrickson, "Human photoreceptor topography," J. Comp. Neurol. **292**, 497–523 (1990).
3. P. K. Ahnelt, H. Kolb, and R. Pflug, "Identification of a subtype of cone photoreceptor, likely to be blue-sensitive, in the human retina," J. Comp. Neurol. **255**, 18–34 (1987).
4. C. A. Curcio, K. A. Allen, K. R. Sloan, C. L. Lerea, J. B. Hurley, I. B. Klock, and A. H. Milam, "Distribution and

morphology of human cone photoreceptors stained with anti-blue," J. Comp. Neurol. **312**, 610–624 (1991).
5. D. R. Williams, D. I. A. MacLeod, and M. M. Hayhoe, "Punctuate sensitivity of the blue-sensitive mechanism," Vision Res. **21**, 1357–1375 (1981).
6. J. A. Castano and H. G. Sperling, "Sensitivity of the blue-sensitive cones across the central retina," Vision Res. **22**, 661–673 (1982).
7. R. E. Marc and H. G. Sperling, "Chromatic organization of primate cones," Science **196**, 454–456 (1977).
8. F. M. de Monasterio, E. P. McCrane, J. K. Newlander, and S. J. Schein, "Density profile of blue-sensitive cones along the horizontal meridian of macaque retina," Invest. Ophthalmol. Visual Sci. **26**, 289–302 (1985).
9. J. D. Mollon and J. K. Bowmaker, "The spatial arrangement of cones in the primate fovea," Nature **360**, 677–679 (1992).
10. O. S. Packer, D. R. Williams, and D. G. Bensinger, "Photopigment transmittance imaging of the primate photoreceptor mosaic," J. Neurosci. **16**, 2251–2260 (1996).
11. H. L. De Vries, "The heredity of the relative number of red and green receptors in the human eye," Genetica (The Hague) **24**, 199–212 (1948).
12. W. A. H. Rushton and H. D. Baker, "Red/green sensitivity in normal vision," Vision Res. **4**, 75–85 (1964).
13. J. J. Vos and P. L. Walraven, "On the derivation of the foveal cone primaries," Vision Res. **11**, 799–818 (1971).
14. R. L. P. Vimal, J. Pokorny, V. C. Smith, and S. K. Shevell, "Foveal cone thresholds," Vision Res. **29**, 61–78 (1989).
15. C. M. Cicerone and J. L. Nerger, "The relative number of long-wavelength-sensitive to middle-wavelength-sensitive cones in the human fovea centralis," Vision Res. **29**, 115–128 (1989).
16. C. M. Cicerone, "Color appearance and the cone mosaic in trichromacy and dichromacy," in *Color Vision Deficiencies*, Y. Ohta, ed. (Kugler & Ghedini, Amsterdam, 1990), pp. 1–2.
17. J. L. Nerger and C. M. Cicerone, "The ratio of L to M cones in the human parafoveal retina," Vision Res. **32**, 879–888 (1992).
18. G. H. Jacobs and J. Neitz, "Electrophysiological estimates of individual variation in the L/M cone ratio," in *Color Vision Deficiencies XI*, B. Drum, ed. (Kluwer Academic, Dordrecht, The Netherlands, 1993), pp. 107–112.
19. P. D. Gowdy and C. M. Cicerone, "The spatial arrangement of L and M cones in the central fovea of the living human eye," Vision Res. **38**, 2575–2589 (1998).
20. A. Roorda and D. R. Williams, "The arrangement of the three cone classes in the living human eye," Nature **397**, 520–522 (1999).
21. S. A. Hagstrom, M. Neitz, and J. Neitz, "Variations in cone populations for red–green color vision examined by analysis of mRNA," NeuroReport **9**, 1963–1967 (1998).
22. J. D. Moreland and A. Cruz, "Colour perception with the peripheral retina," Opt. Acta **6**, 117–151 (1959).
23. M. M. Connors and J. A. S. Kinney, "Relative red–green sensitivity as a function of retinal position," J. Opt. Soc. Am. **52**, 81–84 (1962).
24. R. M. Boynton, W. Schafer, and M. A. Neun, "Hue–wavelength relation measured by color-naming method for three retina locations," Science **146**, 666–668 (1964).
25. H. Uchikawa, P. K. Kaiser, and K. Uchikawa, "Color-discrimination perimetry," Color Res. Appl. **7**, 264–272 (1982).
26. B. R. Wooten and G. Wald, "Color-vision mechanisms in the peripheral retinas of normal and dichromatic observers," J. Gen. Physiol. **61**, 125–145 (1973).
27. U. Stabell and B. Stabell, "Color-vision mechanisms of the extrafoveal retina," Vision Res. **24**, 1969–1975 (1984).
28. U. Stabell and B. Stabell, "Color-vision in the peripheral retina under photopic conditions," Vision Res. **22**, 839–844 (1982).
29. C. Noorlander, J. J. Koenderink, R. J. Den Ouden, and B. W. Edens, "Sensitivity to spatiotemporal colour contrast in the peripheral visual field," Vision Res. **23**, 1–11 (1983).
30. I. Abramov, J. Gordon, and H. Chan, "Color appearance in the peripheral retina: effect of stimulus size," J. Opt. Soc. Am. A **8**, 404–414 (1991).
31. H. Hibino, "Red–green and yellow–blue opponent-color responses as a function of retinal eccentricity," Vision Res. **32**, 1955–1964 (1992).
32. J. L. Nerger, V. Volbrecht, and C. J. Ayde, "Unique hue judgments as a function of test size in the fovea and at 20-deg temporal eccentricity," J. Opt. Soc. Am. A **12**, 1225–1232 (1995).
33. J. A. Van Esch, E. E. Koldenhof, A. J. Van Doorn, and J. J. Koenderink, "Spectral sensitivity and wavelength discrimination of the human peripheral visual field," J. Opt. Soc. Am. A **1**, 443–450 (1984).
34. H. L. De Vries, "Luminosity curve of trichromats," Nature (London) **157**, 736–737 (1946).
35. V. C. Smith and J. Pokorny, "Spectral sensitivity of the foveal cone photopigments between 400 and 500 nm," Vision Res. **15**, 161–171 (1975).
36. A. Eisner and D. I. A. MacLeod, "Blue-sensitive cones do not contribute to luminance," J. Opt. Soc. Am. **70**, 121–123 (1980).
37. J. Pokorny and V. C. Smith, "Evaluation of single pigment shift model of anomalous trichromacy," J. Opt. Soc. Am. **67**, 1196–1209 (1977).
38. J. D. Mollon, "Color vision," Annu. Rev. Psychol. **33**, 41–85 (1982).
39. D. I. A. MacLeod, "Receptoral constraints on color vision," in *Central and Peripheral Mechanisms of Colour Vision*, D. Ottoson and S. Zeki, eds. (Macmillan, London, 1985), pp. 103–116.
40. R. Navarro, P. Artal, and D. R. Williams, "Modulation transfer of the human eye as a function of retinal eccentricity," J. Opt. Soc. Am. A **10**, 201–212 (1993).
41. F. W. Campbell and R. W. Gubisch, "Optical quality of the human eye," J. Physiol. (London) **186**, 558–578 (1966).
42. M. Alpern, "Rhodopsin kinetics in the human eye," J. Physiol. (London) **217**, 447–471 (1971).
43. B. Sakitt, "Counting every quantum," J. Physiol. (London) **223**, 513–529 (1972).
44. W. Makous, "Absolute sensitivity," in *Night Vision*, R. F. Hess, L. T. Sharpe, and K. Nordby, eds. (Cambridge U. Press, Cambridge, UK, 1990), pp. 146–176.
45. J. Nachmias, "On the psychometric function for contrast detection," Vision Res. **21**, 215–223 (1981).
46. D. G. Pelli, "Uncertainty explains many aspects of visual contrast detection and discrimination," J. Opt. Soc. Am. A **2**, 1508–1532 (1985).
47. D. M. Green and J. A. Swets, *Signal Detection Theory and Psychophysics* (Wiley, New York, 1966).
48. D. Jameson and L. M. Hurvich, "Some quantitative aspects of an opponent-colors theory. I. Chromatic responses and spectral saturation," J. Opt. Soc. Am. **45**, 546–552 (1955).
49. D. H. Krantz, "Color measurement and color theory. Opponent-colors theory," J. Math. Psychol. **12**, 304–327 (1975).
50. J. Larimer, D. H. Krantz, and C. M. Cicerone, "Opponent-process additivity. I. Red/green equilibria," Vision Res. **14**, 1127–1140 (1974).
51. T. N. Wiesel and D. H. Hubel, "Spatial and chromatic interactions in the lateral geniculate body of the rhesus monkey," J. Neurophysiol. **29**, 1115–1156 (1966).
52. D. M. Dacey, "Circuitry for color coding in the primate retina," Proc. Natl. Acad. Sci. USA **93**, 582–588 (1996).
53. J. Mollon, "Color vision: opsins and options," Proc. Natl. Acad. Sci. USA **96**, 4743–4745 (1999).
54. R. C. Reid and R. M. Shapley, "Spatial structure of cone inputs to receptive fields in primate lateral geniculate nucleus," Nature **356**, 716–718 (1992).
55. T. Yeh, B. B. Lee, and J. Kremers, "Temporal response of ganglion cells of the macaque retina to cone-specific modulation," J. Opt. Soc. Am. A **12**, 456–464 (1995).
56. W. Paulus and A. Kroger-Paulus, "A new concept of retinal colour coding," Vision Res. **23**, 529–540 (1983).
57. R. L. De Valois and K. K. De Valois, "A multi-stage color model," Vision Res. **33**, 1053–1065 (1993).
58. P. Lennie, P. W. Haake, and D. R. Williams, "The design of

chromatically opponent receptive fields," in *Computational Models of Visual Processing*, M. S. Landy and J. A. Movshon, eds. (MIT Press, Cambridge, Mass., 1991), pp. 71–82.
59. D. J. Calkins, S. J. Schein, Y. Tsukamoto, and P. Sterling, "M and L cones in macaque fovea connect to midget ganglion cells by different numbers of excitatory synapses," Nature **371**, 70–72 (1994).
60. D. M. Dacey and M. R. Petersen, "Dendritic field size and morphology of midget and parasol ganglion cells of the human retina," Proc. Natl. Acad. Sci. USA **89**, 9666–9670 (1992).
61. H. Wässle, B. B. Boycott, and J. Rohrenbeck, "Horizontal cells in the monkey retina: cone connections and dendritic network," Eur. J. Neurosci. **1**, 421–435 (1989).
62. D. M. Purdy, "The Bezold–Brücke phenomenon and contours of constant hue," Am. J. Psychol. **49**, 313–315 (1937).
63. A. L. Nagy and J. L. Zacks, "The effects of psychophysical procedure and stimulus duration in the measurement of Bezold–Brücke hue shifts," Vision Res. **17**, 193–200 (1977).
64. J. S. Werner and B. R. Wooten, "Opponent chromatic mechanisms: relation to photopigments and hue naming," J. Opt. Soc. Am. **69**, 422–434 (1979).
65. J. Larimer, "Red/green opponent colors equilibria measured on chromatic adapting fields: evidence for gain changes and restoring forces," Vision Res. **21**, 501–512 (1981).
66. C. M. Cicerone, "Constraints placed on color vision models by the relative number of different cone classes in human fovea centralis," Farbe **34**, 59–66 (1987).
67. D. I. A. MacLeod and M. A. Webster, "Factors influencing the color matches of normal observers," in *Colour Vision*, J. D. Mollon and L. T. Sharpe, eds. (Academic, London, 1983), pp. 81–92.
68. J. L. Schnapf, T. Kraft, and D. A. Baylor, "Spectral sensitivities of human cone photoreceptors," Nature **325**, 439–441 (1987).
69. S. L. Merbs and J. Nathans, "Absorption spectra of human cone pigments," Nature **356**, 433–435 (1992).
70. E. Zrenner and P. Gouras, "Cone opponency in tonic ganglion cells and its variation with eccentricity in rhesus monkey retina," in *Colour Vision*, J. D. Mollon and L. T. Sharpe, eds. (Academic, London, 1983), pp. 211–224.
71. M. Alpern and E. N. Pugh, Jr., "Variation in the action spectrum of erythrolabe among deuteranopes," J. Physiol. (London) **266**, 613–646 (1977).
72. M. Alpern and T. Wake, "Cone pigments in human deutan colour vision defects," J. Physiol. (London) **266**, 595–612 (1977).
73. J. Neitz and G. H. Jacobs, "Polymorphism in normal human color vision and its mechanisms," Vision Res. **30**, 621–636 (1990).
74. J. Neitz, M. Neitz, and G. H. Jacobs, "More than three different cone pigments among people with normal color vision," Vision Res. **33**, 117–122 (1993).
75. J. K. Bowmaker and H. J. A. Dartnall, "Visual pigments of rods and cones in a human retina," J. Physiol. (London) **298**, 501–511 (1980).
76. H. J. A. Dartnall, J. K. Bowmaker, and J. D. Mollon, "Microspectrophotometry of human photoreceptors," in *Colour Vision*, J. D. Mollon and L. T. Sharpe, eds. (Academic, London, 1983), pp. 69–80.
77. J. D. Mollon and G. Jordan, "Is unique yellow related to the relative numerosity of the L and M cones?" Invest. Ophthalmol. Visual Sci. Suppl. **36**, S189 (1995).
78. E. Miyahara, J. Pokorny, V. C. Smith, R. Baron, and E. Baron, "Color vision in two observers with highly biased LWS/MWS cone ratios," Vision Res. **38**, 601–612 (1998).
79. A. Chaparro, C. F. Stromeyer III, R. E. Kronauer, and R. T. Eskew, Jr., "Separable red–green and luminance detectors for small flashes," Vision Res. **34**, 751–762 (1994).
80. M. J. Sankeralli and K. T. Mullen, "Estimation of the L-, M-, and S-cone weights of the postreceptoral detection mechanisms," J. Opt. Soc. Am. A **13**, 906–915 (1996).
81. J. E. Thornton and E. N. Pugh, Jr., "Red/green opponency at detection threshold," Science **219**, 191–193 (1983).